JPP Journal of Pharmacy and Pharmacology

JPP 2007, 59: 1065–1076

Received November 27, 2006
Accepted April 17, 2007
DOI 10.1211/jpp.59.8.0003
ISSN 0022-3573

Novel, cell-penetrating molecular transporters with flexible backbones and permanently charged side-chains

N. Bodor, É. Tóth-Sarudy, T. Holm, I. Pallagi, E. Vass, P. Buchwald and Ü. Langel

Abstract

Various cell-penetrating peptides have been discovered recently that can translocate across plasma membranes and can even carry large cargo molecules into the cells. Because under physiological conditions most of these peptides carry considerable positive charges due to the presence of basic amino acids such as arginine, we decided to investigate whether molecular transporters composed of permanently charged side-chains also possess such cell penetrating ability. Arginine-rich oligomers that have a backbone with increased flexibility due to incorporation of non-α-amino acids (ε-aminocaproic acid) have been found to be effective molecular transporters. Here, we report the preparation of analogue structures by replacing the arginine residues with the quaternary form of a novel redox amino acid (Nys^+) that contain a trigonelline moiety; it has already been shown possible to replace the original basic amino acid side-chain of neuropeptides without significant activity-loss due to the sufficiently close steric and electronic analogy between the new Nys^+ and the original side-chains (in their protonated form, e.g., Arg^+, Lys^+). A nonamer analogue showed transporter activity resulting in increased cellular uptake in human carcinoma (HeLa) cells.

Center for Drug Discovery, University of Florida, Gainesville, FL, USA

N. Bodor

IVAX Drug Research Institute, Budapest, Hungary

É. Tóth-Sarudy, I. Pallagi

Institute of Chemistry, Department of Organic Chemistry, Eötvös Loránd University, Budapest, Hungary

E. Vass

Molecular and Cellular Pharmacology and Diabetes Research Institute, University of Miami, Miami, FL, USA

P. Buchwald

Dept. of Neurochemistry, Stockholm University, Stockholm, Sweden

T. Holm, Ü. Langel

Correspondence: N. Bodor, Center for Drug Discovery, University of Florida, Health Science Center, P.O. Box 100497, Gainesville, FL 32610-0497, USA. E-mail: bodor@cop.ufl.edu

Acknowledgements and funding: We are grateful to T. Janaky (Szeged, University of Hungary) for the MS spectra, to Z. Zubovics (IDR, Bp.) and M. Hollósi (Eötvös Loránd University, Hungary) for their helpful discussion and to M. Szitás and E. Hivessy for technical assistance. The CD and FTIR spectroscopic studies were supported by the Hungarian Research Foundation (OTKA) Grants T-049792 and T-047186, and the cellular uptake studies by the Swedish Research Council (VR-NT).

Introduction

During the last decade, several cell-penetrating peptides, such as penetratins, Tat-derived peptides or transportan, have been discovered and extensively studied (Lindgren et al 2000; El-Andaloussi et al 2005). Because, apparently, they can not only translocate across the plasma membrane of eukaryotic cells but can also be used for intra- and maybe even transcellular transport of large cargo macromolecules, this might become an important development in the targeting of various biologically and pharmaceutically active compounds. The therapeutic potential of many pharmaceutically active agents is severely limited by their inability to penetrate through the biological barriers that protects tissues and cells from the outside environment. The mechanism by which these peptides translocate is still somewhat obscure, and it might even be different mechanisms depending on peptide or cargo (Zorko & Langel 2005). Most of these compounds carry a considerable positive charge, and a common theory is that they interact with the negatively charged phospholipid heads of the cell membrane (they also seem to interact with heparin sulfate proteoglycans (Tyagi et al 2001)). Peptides derived from HIV-1 Tat protein (e.g. $Tat_{48–60}$), related structures rich in arginine (R) residues (Vivès et al 1997), as well as homopolymers of cationic amino acids in general, and short oligomers of arginine in particular, can also very efficiently translocate and transport their cargo into cells (Rothbard et al 2000, 2002; Wender et al 2000). Most of these peptides are relatively short, usually less than 30 amino acid residues, and the transport they mediate is sometimes independent of receptors and transporters. Such transport could be exploited to increase the bioavailability of drugs in general and of peptides and oligonucleotides in particular, to make possible cellular delivery, and to facilitate transport through biomembranes such as skin and the blood–brain barrier (BBB) (Schwarze et al 1999; Rothbard et al 2000; Rousselle et al 2000; Aarts et al 2002; Bodor & Buchwald 2003a; Deshayes et al 2005).

Rothbard and coworkers have shown the importance of arginine for translocation (Rothbard et al 2000, 2002; Wender et al 2000), and, by using a hepta-arginine peptide, they could deliver ciclosporin through the skin for inhibiting inflammation (Rothbard et al 2000).

The guanidino function in arginine seems to play an important role in the translocation, and this moiety has been reported to form an ideal hydrogen-bonded structure with the phosphate backbone of RNA (Calnan et al 1991). Even a relatively limited number (e.g. 6–7) of guanidine head-groups seems sufficient for efficient cellular uptake, and conformational flexibility of the side-chains seems to have an enhancing effect (Wender et al 2000).

Furthermore, studies with differently spaced arginine side-chains found differential uptake and suggested that increasing the spacing along the backbone of the peptide between the positively charged side-chains could results in greater cellular uptake (Wender et al 2000; Rothbard et al 2002). Glycine has a single methylene between the amino and carboxyl groups, 4-aminobutyric acid has three and 6-aminocaproic acid has five. As the number of methylene units increased from one to three and then further to five, the uptake relative to hepta-L-arginine (R7) increased four, five and sixteen times, respectively. The peptide with ε-aminocaproic acid spacing entered cells more effectively than dexa-L-arginine (R10) (Wright et al 2003). If using (Arg)(*n*) ($n = 4$–16) peptides, the optimal number of arginine residues (*n*) for efficient translocation seems to be around 8.

Previously, in work related to the brain-targeted delivery of neuropeptides, we have shown that in various arginine (Arg, R)-, histidine (His, H)- or lysine (Lys, K)-containing peptides, the original basic amino acid could be replaced by novel redox amino acids (Nys ↔ Nys^+), which contain a 1,4-dihydrotrigonelline ↔ quaternary trigonelline side-chain, without activity-loss due to the sufficiently close steric and electronic analogy between the quaternary form of the redox (Nys^+) and the original side-chains (in their protonated form, Arg^+, Lys^+) (Figure 1) (Chen et al 1998; Bodor & Buchwald 2003b). This analogy is further illustrated in Figure 2 by comparing kyotorphine (Tyr-Arg, YR), an endogenous neuropeptide that exhibits analgesic action through the release of endogenous enkephalin and has analgesic activity about four times larger than Met-enkephalin (Takagi et al 1979), and its redox analogue in its permanently charged form, Tyr-Nys^+. Incorporation of the Nys moiety into the structure of neuropeptides resulted in brain-targeted redox analogue (BTRA) peptides that made possible the non-invasive brain delivery of these important biomolecules in pharmacologically significant amounts (Chen et al 1998; Bodor & Buchwald 2003b), and the peptide with the Nys^+ amino acid, metabolically formed from the originally administered Nys form, produced CNS activity due to the close analogy of its quaternary nicotinamide-containing side-chain with kyotorphine's Arg side-chain, which is always ionized under physiological conditions. Therefore, it seemed reasonable to investigate whether the replacement of the guanidinium headgroups of arginines by such permanently charged Nys^+ redox amino acids still maintains the cell-penetrating activity of the molecular transporter peptides. Other charged analogues have also shown activity (e.g. Fernández-Carneado et al 2005). Certain poly-arginine compounds have been shown to cause inflammatory or toxic responses (Santana et al 1993; Jones et al 2005); these might be avoidable or reducible by different analogues. Here, the synthesis and cell-penetrating ability of a series of such derivatives, incorporating permanently charged $Nys^+(n)$ ($n = 5, 7, 9$) side-chains with equal numbers of aminocaproic acids as spacers, is reported.

Materials and Methods

General methods

All reagents and solvents were purchased from commercial sources and utilized without further purification. The purity of the compounds was tested on TLC plates (silica gel, Merck) with fluorescent indicator (254 nm). Plates were visualized under ultraviolet light and treatment with Cl_2/*o*-tolidine reagent. Solvent systems employed were chloroform–methanol 9:1 (system A), chloroform–methanol 4:1 (system B), ethyl acetate–pyridine–acetic acid–water 15:20:6:11 (system C) or ethyl acetate–pyridine–acetic acid–water 30:20:6:11 (system D). Melting points were determined on a Boetius microscope and are uncorrected. The ^1H and ^{13}C NMR spectra were recorded in dimethyl sulfoxide (DMSO)-d_6

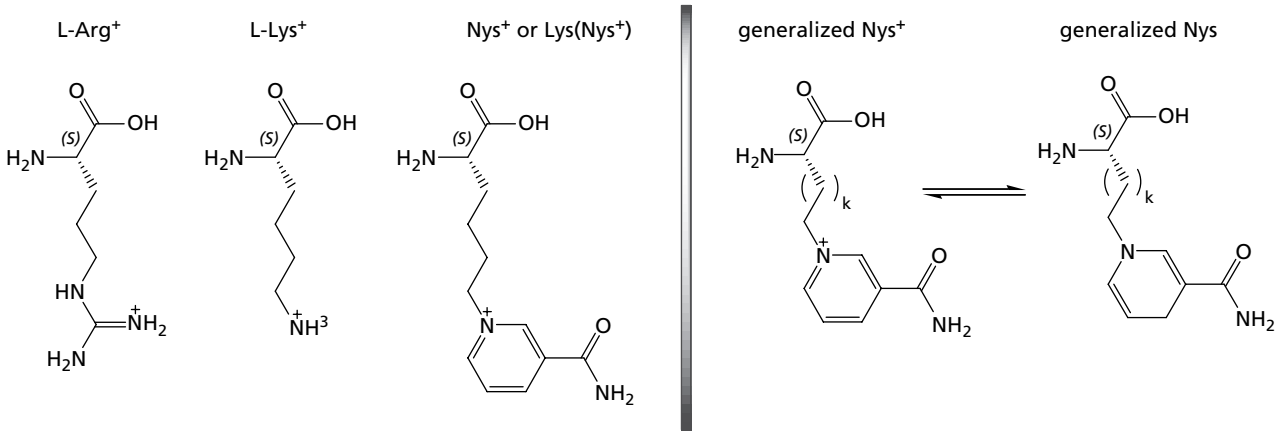

Figure 1 Structure of the Lys(Nys^+) (or simply Nys^+) amino-acid moiety, its analogy to the protonated forms of lysine and arginine and its redox-type transformation into its neutral, dihydro analogue (Nys), which is shown here for a generalized form with adjustable side-chain length (k).

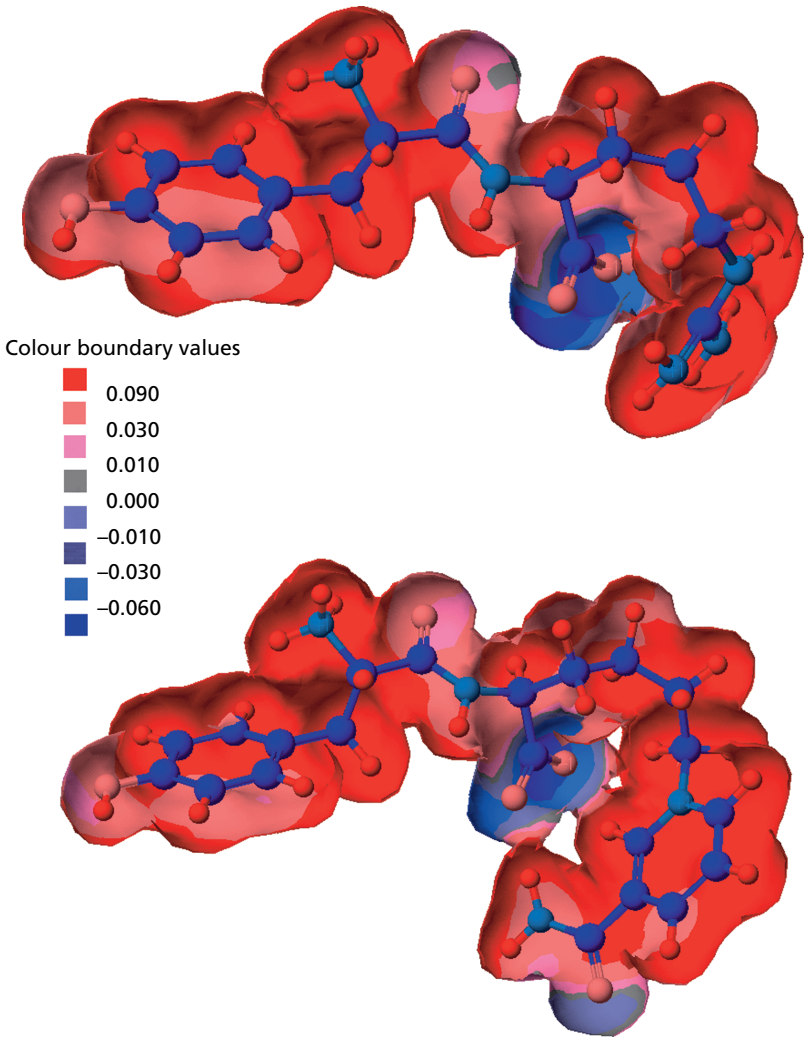

Figure 2 The electronic and steric analogy between Arg and the Nys^+ moiety used in the present molecular transporters, illustrated here with the structures of kyotorphine (Tyr-Arg, top structure) and the quaternary for of its brain-targeted redox analogue (BTRA), Tyr-Nys^+ (bottom structure). AM1-optimized structures and electron-isodensity surfaces (0.01 electron/$Å^3 \approx 0.0015$ electron/$bohr^3$) shown; the colour-code changes gradually from blue, which corresponds to the more negative regions, to red, which corresponds to the more positive regions along the surface.

solution using a Bruker Avance-500 spectrometer at frequencies of 500 and 126 MHz, respectively. For structure elucidation, one-dimensional ^1H, ^{13}C, DEPT-135, sel. TOCSY, sel. NOESY, two-dimensional ^1H, ^1H-COSY, ^1H, ^1H-TOCSY, ^1H, ^{13}C-HSQC and ^1H, ^{13}C-HMBC measurements were run. Temperatures of the ^1H NMR spectra were investigated in the range of 300–383 K. Chemical shifts are given on the δ-scale and were references to TMS. Mass spectra utilizing electrospray ionization (ESI-MS) were recorded at the mass spectrometry laboratory at Szeged University utilizing a Finnigan TSQ 7000 triple Quad mass spectrometer. All compounds gave satisfactory elemental analysis values.

General procedure A: deprotection of BOC-amides

Trifluoracetic acid (4 mL) was added slowly at 5°C to a solution of BOC-amide (0.3 mmol) in CH_2Cl_2 (12 mL) and the mixture was stirred for 2 h at room temperature. The desired product was obtained from the reaction mixture by evaporation of the solvent and was used without further purification.

General procedure B: removal of the benzyloxy carbonyl group

To a solution of the derivative (0.08 mmol) in acetic acid (20 mL) was added Pd/C (10% Pd, 300 mg) followed by introduction of hydrogen gas (1 atm, balloon). The reaction mixture was stirred at room temperature until TLC showed complete consumption of the starting material. The reaction mixture was then filtered and the solvent was removed in-vacuo to give the desired product, which was used without further purification.

General procedure C: amide coupling

To a stirred solution of the deprotected amide (see procedure A) (0.33 mmol) in DMF (15 mL), the 2,4,5-trichlorophenyl ester

(TCP) (**5, 10** or **28**) (0.4 mmol) in DMF (1 mL) and triethylamine (TEA) (1.3 mmol) were added at room temperature. The reaction mixture was stirred until TLC revealed the complete consumption of the starting amine. The reaction mixture was then stirred with water (80 mL) and the precipitate was collected by filtration, washed twice with ethyl acetate, dried in-vacuo until constant weight and used without further purification.

General procedure D: formation of poly (Nys$^+$) side chain by Zincke reaction

The Zincke reaction is an organic reaction in which a pyridine is transformed into a pyridinium salt by reaction with 1-chloro-2, 4-dinitrobenzene and a primary amine. A mixture of nicotinamide and 1-chloro-2,4-dinitrobenzene was heated at 100°C for 1 h. After cooling, the product was dissolved in methanol and poured into ether. The *N*-(2,4-dinitrophenyl)-nicotinamide chloride (Zincke reagent) was filtered as pale yellow crystals. A solution of the salt (0.5 mmol) in methanol (2 mL) was slowly added to a stirred solution of 0.05–0.10 mmol of compounds **18, 19, 20** and **32**, respectively in methanol (5 mL) at 10°C. The obtained red solution was stirred under reflux for 5 h. The organic solvent was removed in-vacuo. The crude product was purified by column chromatography on Sephadex LH-20 in methanol with UV detection at 255 nm, flow rate 1 mL min^{-1}.

General procedure E: fluorescein labelling of compounds

To the solution of deprotected (see procedure A) compounds (0.04 mmol) in 900 μL of anhydrous DMSO, the solution of 23.3 mg (0.06 mmol) of fluorescein isothiocyanate in 200 μL of anhydrous DMSO was added at pH 8.5 (80 μL TEA). The mixture was stirred at room temperature in the dark for 24 h. After concentration in-vacuo, the residue was purified by column chromatography on Sephadex LH-20 in methanol with UV detection, flow rate 1 mL min^{-1}.

*BOC-Lys(Z)-aca-OTCP (**5**)*
BOC-Lys(Z)-aca-OH (0.986 g, 2 mmol) and 2,4,5-trichlorophenol (0.480 g, 2.4 mmol) dissolved in THF (25 mL) were condensed in the presence of DCC (0.494 g, 2.4 mmol). The crude product was purified by column chromatography on Kieselgel-60 eluting with ethyl acetate-n-hexane 2:1. Yield 0.65 g (65%). Mp: 60 °C. Anal. ($C_{31}H_{41}Cl_3N_3O_7$) C, H, N. ^{1}H NMR (500 MHz, DMSO-d_6): δ 1.36 (9H, s, Bu^t), 1.1–1.8 (6H + 6H, m, HNCH$_2$(CH_2)$_3$ and CH(CH_2)$_3$), 2.61 (2H, t, CH_2COOAryl), 2.9–3.2 (4H, m, HNCH_2), 3.81 (1H, m, NHCHCO), 4.9–5.1 (2H, s, br, OCH_2Ph), 6.69 (1H, d, Bu^{t}OCONHCH), 7.18 (1H, t, OCONHCH$_2$), 7.2–7.4 (5H, Ph H), 7.72 (1H, t, CHCONHCH$_2$), 7.78/8.01 (1H + 1H, s, Aryl H). ^{13}C NMR (125 MHz, DMSO): δ 28.1 (C($CH3$)$_3$), 54.3 (HNCHCONH), 65.0, (OCH_2Ph), 77.9 (C(CH3)$_3$), 155.2 (Bu^{t}OCONH), 156.0 (HNCOOCH$_2$Ph), 170.4 (CH$_2$$CO$OAr), 171.9 ($CO$NHCH$_2$).

*BOC-aca-Lys(Z)-aca-OTCP (**10**)*
BOC-aca-Lys(Z)-aca-OH (0.74 g, 1.2 mmol) and 2,4,5-trichlorophenol (0.256 g, 1.3 mmol) dissolved in THF (20 mL) were condensed in the presence of DCC (0.265 g, 1.3 mmol) in the usual manner. The crude product was purified by Kieselgel-60 chromatography using ethyl acetate–n-hexane 4:1. Yield 0.64 g (67%). Mp: 97°C. Anal. ($C_{37}H_{52}Cl_3N_4O_8$) C, H, N. ^{1}H NMR (500 MHz, DMSO-d_6): δ 1.36 (9H, s, Bu^t), 1.1–1.8 (12H + 6H, m, HNCH$_2$(CH_2)$_3$ and CH(CH_2)$_3$), 2.09 (2H, m, CH$_2$CO), 2.63 (2H, m, CH_2COOAryl), 2.8–3.1 (6H, m, HNCH_2), 4.15 (1H, m, NHCHCO), 4.9–5.1 (2H, s, br, OCH_2Ph), 7.2–7.4 (5H, m, Ph H), 7.77/8.01 (1H + 1H, s, Aryl H). ^{13}C NMR (125 MHz, DMSO): δ 28.2 (C($CH3$)$_3$), 52.4 (HNCHCONH), 65.0, (OCH_2Ph), 77.2 (C(CH3)$_3$), 155.5 (Bu^{t}OCONH), 156.0 (HNCOOCH$_2$Ph), 170.4 (CH$_2$$CO$OAr), 171.6 ($CO$NHCH$_2$), 172.0 (CH$_2$$CO$NH).

*BOC-Lys(Z)-Lys(Z)-aca-OTCP (**28**)*
BOC-Lys(Z)-Lys(Z)-aca-OH (0.9 g, 1 mmol) and 2,4,5-trichlorophenol (0.24 g, 1.2 mmol) dissolved in THF (12 mL) were condensed in the presence of DCC (0.247 g, 1.2 mmol) in the usual manner. The crude solid was chromatographed on Kieselgel-60 (eluent ethyl acetate–n-hexane 4:1). Yield 0.84 g (76%). Mp: 127°C. Anal. ($C_{45}H_{59}Cl_3N_5O_{10}$) C, H, N. ^{1}H NMR (500 MHz, DMSO-d_6): δ 1.36 (9H, s, Bu^t), 1.1–1.8 (6H + 12H, m, HNCH$_2$(CH_2)$_3$ and CH(CH_2)$_3$), 2.61 (2H, t, CH_2COOAryl), 2.9–3.2 (6H, m, HNCH_2), 3.84 (1H, m, Bu^{t}OCONHCH), 4.15 (1H, m, NHCHCO), 4.9–5.1 (4H, s, br, OCH_2Ph), 6.88 (1H, d, Bu^{t}OCONHCH), 7.66 (1H, d, NHCHCO), 7.2–7.4 (10H, Ph H), 7.77/8.01 (1H + 1H, s, Aryl H). ^{13}C NMR (125 MHz, DMSO): δ 28.1 (C($CH3$)$_3$), 52.2 (HNCHCONH), 54.5 (Bu^{t}OCONHCH), 65.0 (OCH_2Ph), 78.1 (C(CH3)$_3$), 155.4 (Bu^{t}OCONH), 156.0 (HNCOOCH$_2$Ph), 170.4 (CH$_2$$CO$OAr), 171.2 ($CO$NHCH$_2$), 171.8 (CH$CO$NH).

*BOC-Lys(Z)-aca-Lys(Z)-NH$_2$ (**7**)*
General procedure C was followed starting with ester **5** (1.7 g, 2.5 mmol) and amine **6** (0.56 g, 2 mmol). Yield 2.07 g (83%). Mp: 124°C, R_f = 0.50 (System A). Anal. ($C_{39}H_{58}N_6O_9$) C, H, N. ^{1}H NMR (500 MHz, DMSO-d_6): δ 1.36 (9H, s, Bu^t), 1.1–1.7 (6H + 12H, m, HNCH$_2$(CH_2)$_3$ and CH(CH_2)$_3$), 2.09 (2H, t, CH$_2$CO), 2.9–3.1 (6H, m, HNCH_2), 3.81 (1H, m, Bu^{t}OCONHCH), 4.15 (1H, m, NHCHCO), 4.9–5.1 (4H, s, br, OCH_2Ph), 6.66 (1H, d, Bu^{t}OCONHCH), 6.90/7.25 (1H + 1H, s, CONH$_2$) 7.2–7.3 (5H, m, Ph H), 7.73 (1H, d, HNCHCONH$_2$).

*BOC-Lys(Z)-aca-Lys(Z)-aca-Lys(Z)-NH$_2$ (**8**)*
General procedure C was followed starting with ester **5** (1 g, 1.5 mmol) and the crude amine (0.785 g, 1.2 mmol) obtained by deprotection of **7** according to procedure A. Yield 1.13 g (87%). Mp: 167°C, R_f = 0.44 (System A). Anal. ($C_{59}H_{87}N_9O_{13}$) C, H, N. ^{1}H NMR (500 MHz, DMSO-d_6): δ 1.36 (9H, s, Bu^t), 1.1–1.7 (12H + 18H, m, HNCH$_2$(CH_2)$_3$ and CH(CH_2)$_3$), 2.09 (4H, m, CH$_2$CO), 2.9–3.1 (10H, m, HNCH_2), 3.82 (1H, m, Bu^{t}OCONHCH), 4.15 (2H, m, NHCHCO), 4.9–5.1 (6H, s, br, OCH_2Ph), 6.68 (1H, d, Bu^{t}OCONHCH), 7.2–7.4 (15H, m, Ph H).

*BOC-Lys(Z)-aca-[Lys(Z)-aca]$_2$-Lys(Z)-NH$_2$ (**9**)*
General procedure C was followed starting with ester **5** (0.80 g, 1.2 mmol) and the crude amine (1 g, 1 mmol)

obtained by deprotection of **8** according to procedure A. Yield 1.13 g (78%). Mp: 190°C, R_f = 0.60 (System A). Anal. ($C_{79}H_{116}N_{12}O_{17}$) C, H, N. ^{1}H NMR (500 MHz, DMSO-d_6): δ 1.36 (9H, s, Bu^t), 1.1–1.7 (18H + 24H, m, HNCH$_2$(CH_2)$_3$ and CH(CH_2)$_3$), 2.09 (6H, m, CH_2CO), 2.8–3.1 (14H, m, HNCH_2), 3.82 (1H, m, Bu^{t}OCONHCH), 4.15 (3H, m, NHCHCO), 4.99 (8H, s, br, OCH_2Ph), 7.2–7.4 (20H, m, Ph H).

*BOC-aca-[Lys(Z)-aca]$_4$-Lys(Z)-NH$_2$ (**11**)*

General procedure C was followed starting with ester **10** (0.58 g, 0.73 mmol) and the crude amine (0.92 g, 0.6 mmol) obtained by deprotection of **9** according to procedure A. Yield 0.89 g (69%). Mp: 198–200°C, R_f = 0.60 (System B). Anal. ($C_{105}H_{156}N_{16}O_{22}$) C, H, N. ^{1}H NMR (500 MHz, DMSO-d_6): δ 1.35 (9H, s, Bu^t), 1.1–1.7 (30H + 30H, m, HNCH$_2$(CH_2)$_3$ and CH(CH_2)$_3$), 2.09 (10H, m, CH_2CO), 2.85 (2H, q, Bu^{t}OCONHCH_2), 2.9–3.1 (20H, m, HNCH_2), 4.15 (5H, m, NHCHCO), 4.99 (10H, s, br, OCH_2Ph), 6.69 (1H, t, br, Bu^{t}OCONHCH$_2$) 7.2–7.4 (25H, m, Ph H). ^{13}C NMR (125 MHz, DMSO): δ 28.2 (C($CH3$)$_3$), 39.8 (Bu^{t}OCONHCH_2), 52.1 (CHCONH$_2$), 52.3 (HNCHCO), 65.1, OCH_2Ph), 77.3 (C(CH3)$_3$), 155.5 (Bu^{t}OCONH), 156.0 (HNCOOCH$_2$Ph), 171.5 (HNCHCO), 173.9 (CONH$_2$).

*BOC-Lys(Z)-aca-[Lys(Z)-aca]$_3$-Lys(Z)-NH$_2$ (**12**)*

General procedure C was followed starting with ester **5** (0.27 g, 0.4 mmol) and the crude amine (0.5 g, 0.35 mmol) obtained by deprotection of **9** according to procedure A. Yield 0.51 g (77%). Mp: 193°C, R_f = 0.65 (System B). Anal. ($C_{99}H_{145}N_{15}O_{21}$) C, H, N. ^{1}H NMR (500 MHz, DMSO-d_6): δ 1.36 (9H, s, Bu^t), 1.1–1.7 (24H + 30H, m, HNCH$_2$(CH_2)$_3$ and CH(CH_2)$_3$), 2.08 (8H, m, CH_2CO), 2.9–3.1 (18H, m, HNCH_2), 3.81 (1H, m, Bu^{t}OCONHCH), 4.15 (4H, m, NHCHCO), 4.9–5.1 (10H, s, br, OCH_2Ph), 6.66 (1H, d, Bu^{t}OCONHCH), 6.90/7.25 (1H + 1H, s, CONH$_2$) 7.2–7.4 (25H, m, Ph H).

*BOC-Lys(Z)-aca-[Lys(Z)-aca]$_4$-Lys(Z)-NH$_2$ (**13**)*

General procedure C was followed starting with ester **5** (0.35 g, 0.5 mmol) and the crude amine (0.711 g, 0.4 mmol) obtained by deprotection of **12** according to procedure A. Yield 0.78 g (87%). Mp: 201°C, R_f = 0.55 (System B). Anal. ($C_{119}H_{174}N_{18}O_{25}$). C, H, N. ^{1}H NMR (500 MHz, DMSO-d_6): δ 1.36 (9H, s, Bu^t), 1.1–1.7 (30H + 36H, m, HNCH$_2$(CH_2)$_3$ and CH(CH_2)$_3$), 2.08 (10H, m, CH_2CO), 2.9–3.1 (22H, m, HNCH_2), 3.81 (1H, m, Bu^{t}OCONHCH), 4.15 (5H, m, NHCHCO), 4.9–5.1 (12H, s, br, OCH_2Ph), 6.66 (1H, d, Bu^{t}OCONHCH), 6.90/7.25 (1H + 1H, s, CONH$_2$), 7.2–7.4 (30H, m, Ph H).

*BOC-aca-[Lys(Z)-aca]$_6$-Lys(Z)-NH$_2$ (**14**)*

General procedure C was followed starting with ester **10** (0.277 g, 0.35 mmol) and the crude amine (0.5 g, 0.23 mmol) obtained by deprotection of **13** according to procedure A. Yield 0.42 g (66%). Mp: 189°C, R_f = 0.35 (System B). Anal. ($C_{145}H_{214}N_{22}O_{30}$) C, H, N. ^{1}H NMR (500 MHz, DMSO-d_6): δ 1.35 (9H, s, Bu^t), 1.1–1.7 (42H + 42H, m, HNCH$_2$(CH_2)$_3$ and CH(CH_2)$_3$), 2.08 (14H, m, CH_2CO), 2.88 (2H, m, Bu^{t}OCONHCH_2), 2.9–3.1 (28H, m, HNCH_2), 4.15 (7H, m, NHCHCO), 4.9–5.1 (14H, s, br, OCH_2Ph), 6.70 (1H, br, Bu^{t}OCONHCH$_2$), 7.2–7.4 (35H, m, Ph H).

*BOC-Lys(Z)-aca-[Lys(Z)-aca]$_5$-Lys(Z)-NH$_2$ (**15**)*

General procedure C was followed starting with ester **5** (0.24 g, 0.35 mmol) and the crude amine (0.61 g, 0.28 mmol) obtained by deprotection of **13** according to procedure A. Yield 0.68 g (91%). Mp: 208°C, R_f = 0.7 (System B). Anal. ($C_{139}H_{203}N_{21}O_{29}$) C, H, N. ^{1}H NMR (500 MHz, DMSO-d_6): δ 1.36 (9H, s, Bu^t), 1.1–1.7 (36H + 42H, m, HNCH$_2$(CH_2)$_3$ and CH(CH_2)$_3$), 2.09 (12H, m, CH_2CO), 2.8–3.1 (26H, m, HNCH_2), 3.82 (1H, m, Bu^{t}OCONHCH), 4.15 (6H, m, NHCHCO), 4.9–5.1 (14H, s, br, OCH_2Ph), 6.66 (1H, d, Bu^{t}OCONHCH), 6.90/7.23 (1H + 1H, s, CONH$_2$), 7.2–7.4 (35H, m, Ph H). ^{13}C NMR (125 MHz, DMSO): δ 28.1 (C($CH3$)$_3$), 52.1 (CHCONH$_2$), 52.3 (HNCHCO), 54.2 (Bu^{t}O-CONHCHCO) 65.0 (OCH_2Ph), 77.8 (C(CH3)$_3$), 156.0 (HNCOOCH$_2$Ph), 171.5 (NHCHCO), 171.8 (Bu^{t}ONH-CHCO), 171.9 (CH$_2CO$NH).

*BOC-Lys(Z)-aca-[Lys(Z)-aca]$_6$-Lys(Z)-NH$_2$ (**16**)*

General procedure C was followed starting with ester **5** (0.13 g, 0.19 mmol) and the crude amine (0.41 g, 0.16 mmol) obtained by deprotection of **15** according to procedure A. Yield 0.44 g (90%). Mp: 215°C, R_f = 0.6 (System B). Anal. ($C_{159}H_{232}N_{24}O_{33}.H_2O$) C, H, N. ^{1}H NMR (500 MHz, DMSO-d_6): δ 1.35 (9H, s, Bu^t), 1.1–1.7 (42H + 48H, m, HNCH$_2$(CH_2)$_3$ and CH(CH_2)$_3$), 2.09 (14H, m, CH_2CO), 2.8–3.1 (30H, m, HNCH_2), 3.80 (1H, m, Bu^{t}OCONHCH), 4.15 (6H, m, NHCHCO), 4.9–5.1 (16H, s, br, OCH_2Ph), 6.72 (1H, d, Bu^{t}OCONHCH), 7.2–7.4 (40H, m, Ph H).

*BOC-aca-[Lys(Z)-aca]$_8$-Lys(Z)-NH$_2$ (**17**)*

General procedure C was followed starting with ester **10** (0.16 g, 0.2 mmol) and the crude amine (0.41 g, 0.14 mmol) obtained by deprotection of **16** according to procedure A. Yield 0.44 g (89%). Mp: 217°C, R_f = 0.40 (System B). Anal. ($C_{185}H_{272}N_{28}O_{38}.2H_2O$) C, H, N. ^{1}H NMR (500 MHz, DMSO-d_6): δ 1.35 (9H, s, Bu^t), 1.1–1.7 (54H + 54H, m, HNCH$_2$(CH_2)$_3$ and CH(CH_2)$_3$), 2.08 (18H, m, CH_2CO), 2.86 (2H, q, Bu^{t}OCONHCH_2), 2.9–3.1 (36H, m, HNCH_2), 4.15 (9H, m, NHCHCO), 4.9–5.1 (18H, s, br, OCH_2Ph), 6.72 (1H, br, Bu^{t}OCONHCH$_2$), 7.2–7.4 (45H, m, Ph H).

*BOC-aca-[Lys-aca]$_8$-Lys-NH$_2$ (**20**)*

General procedure B was followed starting with protected polyamine **17** (0.26 g, 0.075 mmol) and reaction time of 6 h. After work up, the desired product **20** was obtained as a white power (0.21 g, 0.075 mmol, yield quantitative). Mp: 135–138°C, R_f = 0.6 (System C). Anal. ($C_{113}H_{218}N_{28}O_{20}$·9$CH_3$COOH) C, H, N. ^{1}H NMR (500 MHz, DMSO-d_6): δ 1.38 (9H, s, Bu^t), 1.1–1.7 (54H + 54H, m, HNCH$_2$(CH_2)$_3$ and CH(CH_2)$_3$), 1.87 (35H, s, br, CH_3CO), 2.10 (18H, m, CH_2CO), 2.58/2.9–3.1 (26H, m, NH$_2CH_2$and NHCH_2), 2.89 (2H, q, Bu^{t}OCONHCH_2), 4.18 (9H, m, NHCHCO).

*BOC-aca-[Lys(Nys$^+$)-aca]$_4$-Lys(Nys$^+$)-NH$_2$ (**21**)*

General procedure D was followed with N-(2,4-dinitrophenyl)-pyridinium chloride (0.3 g, 0.92 mmol) and polyamine

18 (0.15 g, 0.11 mmol). Yield 0.143 g (62%). Mp: 134°C. Anal. ($C_{95}H_{145}Cl_5N_{21}O_{17}$) C, H, N. ^{1}H NMR (500 MHz, DMSO-d_6): δ 1.36 (9H, s, Bu^t), 1.1–1.7 (30H + 20H, m, HNCH$_2$(*CH$_2$*)$_3$ and CH(*CH$_2$*)$_2$), 1.95 (10H, *CH$_2$*(CH$_2$)$_2$CH), 2.14 (10H, m, CH$_2$CO), 2.86 (2H, q, Bu^{t}OCONHC*H$_2$*), 2.9–3.1 (10H, m, HN*CH$_2$*), 4.15 (5H, m, NH*CH*CO), 4.66 (10H, s, br, *CH$_2$*(CH$_2$)$_3$CH), 6.74 (1H, t, br, Bu^{t}OCO*NH*CH$_2$), 6.98/7.28 (1H + 1H, s, CHCO*NH$_2$*), 8.27 (5H, dd, pyridine), 8.98 (5H, br, pyridine), 9.24 (5H, br, pyridine), 9.63 (5H, d, pyridine).

*BOC-aca-[Lys(Nys$^+$)-aca]$_6$-Lys(Nys$^+$)-NH$_2$ (**22**)*

General procedure D was followed with *N*-(2,4-dinitrophenyl)-pyridinium chloride (0.17 g, 0.52 mmol) and polyamine **19** (0.15 g, 0.06 mmol). Yield 0.153 g (82%). Mp: 127°C. Anal. ($C_{131}H_{200}Cl_7N_{29}O_{23}.H_2O$) C, H, N. ^{1}H NMR (500 MHz, DMSO-d_6): δ 1.36 (9H, s, Bu^t), 1.1–1.7 (42H + 28H, m, HNCH$_2$(*CH$_2$*)$_3$ and CH(*CH$_2$*)$_2$), 1.97 (14H, *CH$_2$*(CH$_2$)$_2$CH), 2.14 (14H, m, CH$_2$CO), 2.85 (2H, q, Bu^{t}OCONHC*H$_2$*), 2.9–3.1 (12H, m, HN*CH$_2$*), 4.20 (7H, m, NH*CH*CO), 4.67 (14H, s, br, *CH$_2$*(CH$_2$)$_3$CH), 6.74 (1H, t, br, Bu^{t}OCO*NH*CH$_2$), 6.98/7.41 (1H + 1H, s, CHCO*NH$_2$*), 8.27 (7H, dd, pyridine), 8.98 (7H, m, pyridine), 9.24 (7H, m, pyridine), 9.65 (7H, m, pyridine).

*BOC-aca-[Lys(Nys$^+$)-aca]$_8$-Lys(Nys$^+$)-NH$_2$ (**23**)*

General procedure D was followed with *N*-(2,4-dinitrophenyl)-pyridinium chloride (0.246 g, 0.76 mmol) and polyamine **20** (0.18 g, 0.08 mmol). After work up, the desired product **23** was obtained as a yellow foam. Yield 0.17 g (61%). Mp: 145°C. Anal. ($C_{167}H_{262}Cl_9N_{37}O_{29}$) C, H, N. ^{1}H NMR (500 MHz, DMSO-d_6): δ 1.35 (9H, s, Bu^t), 1.1–1.7 (54H + 36H, m, HNCH$_2$(*CH$_2$*)$_3$ and CH(*CH$_2$*)$_2$), 1.97 (18H, *CH$_2$*(CH$_2$)$_2$CH), 2.08 (18H, m, CH$_2$CO), 2.85 (2H, q, Bu^{t}OCONHC*H$_2$*), 2.9–3.1 (18H, m, HN*CH$_2$*), 4.20 (9H, m, NH*CH*CO), 4.67 (18H, s, br, *CH$_2$*(CH$_2$)$_3$CH), 6.73 (1H, t, br, Bu^{t}OCO*NH*CH$_2$), 6.97/7.41 (1H + 1H, s, CHCO*NH$_2$*), 8.26 (9H, dd, pyridine), 8.98 (9H, m, pyridine), 9.26 (9H, m, pyridine), 9.69 (9H, m, pyridine).

*HCl.H-aca-[Lys(Nys$^+$)-aca]$_8$-Lys(Nys$^+$)-NH$_2$ (**26**)*

General procedure A was followed starting with protected **23** (0.17 g, 0.047 mmol) using CH_2Cl_2 (12 mL) trifluoroacetic acid (4 mL) and a reaction time of 2 h. After concentration of the solvent in-vacuo, treatment with 1 M hydrogen chloride in EtOH, the desired product **26** was obtained as a yellow amorphous foam (0.165 g, 0.047 mmol, quantitative yield). Mp: 60°C. Anal. ($C_{162}H_{254}Cl_9N_{37}O_{27}$.HCl) C, H, N.

*BOC-Lys(Z)-Lys(Z)-aca-Lys(Z)-Lys(Z)-NH$_2$ (**29**)*

General procedure C was followed starting with ester **28** (0.49 g, 0.52 mmol) and amine **27** (0.368 g, 0.48 mmol) in THF. After work up, the crude solid was taken up in $CHCl_3$–MeOH 9:1 and passed through a short column of silica gel. Removal of the solvent in-vacuo gave the desired product **29** as a white power 0.5 g (68%). Mp: 190°C, R_f = 0.45 (system A). Anal. ($C_{67}H_{94}N_{10}O_{15}$) C, H, N. ^{1}H NMR (500 MHz, DMSO-d_6): δ 1.36 (9H, s, Bu^t), 1.1–1.7 (6H + 24H, m, HNCH$_2$(*CH$_2$*)$_3$ and CH(*CH$_2$*)$_3$), 2.09 (2H, m, CH$_2$CO), 2.9–3.1 (10H, m, HN*CH$_2$*), 3.84 (1H, m, Bu^{t}OCONHC*H*), 4.15 (3H, m, NH*CH*CO), 4.9–5.1 (8H, s, br, O*CH$_2$*Ph), 6.88 (1H, d, Bu^{t}OCO*NH*CH), 6.96/7.24 (1H + 1H, s, CONH$_2$), 7.2–7.4 (20H, m, Ph H), 7.81 (1H, t, CHCO*NH*CH$_2$).

*BOC-Lys(Z)-Lys(Z)-aca-Lys(Z)-Lys(Z)-aca-Lys(Z)-Lys(Z)-NH$_2$ (**30**)*

General procedure C was followed in THF (13 mL) starting with ester **28** (0.42 g, 0.45 mmol) and the crude amine (0.5 g, 0.42 mmol) obtained by deprotection of **29** according to procedure A. After work up, the crude solid was taken up in $CHCl_3$–MeOH 9:1 and filtered. Removal of the solvent in vacuo gave the desired product **30**. Yield 0.39 g (53%). Mp: 183°C, R_f = 0.35 (system A). Anal. ($C_{101}H_{141}N_{15}O_{22}$) C, H, N. ^{1}H NMR (500 MHz, DMSO-d_6): δ 1.36 (9H, s, Bu^t), 1.1–1.7 (12H + 36H, m, HNCH$_2$(*CH$_2$*)$_3$ and CH(*CH$_2$*)$_3$), 2.09 (4H, m, CH$_2$CO), 2.8–3.1 (16H, m, HN*CH$_2$*), 3.85 (1H, m, Bu^{t}OCONHC*H*), 4.15 (5H, m, NH*CH*CO), 4.9–5.1 (12H, s, br, O*CH$_2$*Ph), 6.88 (1H, d, Bu^{t}OCO*NH*CH), 6.97/7.24 (1H + 1H, s, CONH$_2$), 7.2–7.4 (30H, m, Ph H).

*BOC-aca-Lys(Z)-aca-[Lys(Z)-Lys(Z)-aca]$_2$-Lys(Z)-Lys(Z)-NH$_2$ (**31**)*

General procedure C was followed starting with ester **10** (0.171 g, 0.2 mmol) and the crude amine (0.33 g, 0.18 mmol) obtained by deprotection of **30** according to procedure A. Yield 0.3 g (72%). Mp: 185°C, R_f = 0.65 (system D). Anal. ($C_{127}H_{181}N_{19}O_{27}$) C, H, N. ^{1}H NMR (500 MHz, DMSO-d_6): δ 1.35 (9H, s, Bu^t), 1.1–1.7 (24H + 42H, m, HNCH$_2$(*CH$_2$*)$_3$ and CH(*CH$_2$*)$_3$), 1.9–2.2 (8H, m, CH$_2$CO), 2.85 (2H, q, Bu^{t}OCONHC*H$_2$*), 2.9–3.1 (20H, m, HN*CH$_2$*), 4.15 (7H, m, NH*CH*CO), 4.98 (14H, s, br, O*CH$_2$*Ph), 6.68 (1H, br, Bu^{t}OCO*NH*CH$_2$), 7.2–7.4 (35H, m, Ph H).

*BOC-aca-Lys(Nys$^+$)-aca-[Lys(Nys$^+$)-Lys(Nys$^+$)-aca]$_2$-Lys(Nys$^+$)-Lys(Nys$^+$)-NH$_2$ (**33**)*

General procedure D was followed with *N*-(2,4-dinitrophenyl)-pyridinium chloride (0.24 g, 0.75 mmol) and polyamine **32** (0.15 g, 0.1 mmol). Yield 0.16 g (64%). Mp: 150°C. Anal. ($C_{113}H_{167}Cl_7N_{26}O_{20}.H_2O$) C, H, N. ^{1}H NMR (500 MHz, DMSO-d_6): δ 1.1–1.7 (24H + 28H, m, HNCH$_2$(*CH$_2$*)$_3$ and CH(*CH$_2$*)$_2$), 1.97 (14H, *CH$_2$*(CH$_2$)$_2$CH), 2.09 (8H, m, CH$_2$CO), 2.85 (2H, q, Bu^{t}OCONHC*H$_2$*), 2.9–3.1 (8H, m, HN*CH$_2$*), 4.21 (7H, m, NH*CH*CO), 4.67 (14H, s, br, *CH$_2$*(CH$_2$)$_3$CH), 6.72 (1H, t, br, Bu^{t}OCO*NH*CH$_2$), 7.03/7.44 (1H + 1H, s, CHCO*NH$_2$*), 8.26 (7H, dd, pyridine), 8.99 (7H, m, pyridine), 9.28 (7H, m, pyridine), 9.68 (7H, m, pyridine).

*Fluorescein-aca-[Lys(Nys$^+$)-aca]$_4$-Lys(Nys$^+$)-NH$_2$ (**1**)*

General procedure E was followed with fluorescein isothiocyanate (23 mg, 0.06 mmol) and amine **24** (0.08 g, 0.04 mmol). Yield 0.071 g (75%). Mp: 150°C. Anal. ($C_{111}H_{148}Cl_5N_{22}O_{20}S$) C, H, N. ^{1}H NMR (500 MHz, DMSO-d_6): δ 1.1–1.7 (30H + 20H, m, HNCH$_2$(*CH$_2$*)$_3$ and CH(*CH$_2$*)$_2$), 1.96 (10H, *CH$_2$*(CH$_2$)$_2$CH), 2.08 (10H, m, CH$_2$CO), 2.9–3.1 (8H, m, HN*CH$_2$*), 3.45 (2H, m, SCNHC*H$_2$*), 4.19 (5H, m, NH*CH*CO), 4.65 (10H, s, br, *CH$_2$*(CH$_2$)$_3$CH), 6.5–6.6 (4H, m, aryl H), 6.68 (2H, s, br, aryl H), 7.14 (1H, d, aryl H), 8.26 (5H, dd, pyridine), 8.98 (5H, br, pyridine), 9.23 (5H, br, pyridine), 9.60 (5H, br, pyridine).

*Fluorescein-aca-[Lys(Nys$^+$)-aca]$_6$-Lys(Nys$^+$)-NH$_2$ (**2**)*
General procedure E was followed with fluorescein isothiocyanate (30 mg, 0.078 mmol) and amine **25** (0.14 g, 0.052 mmol). Yield 0.07 g (67%). Mp: 160–163°C. Anal. ($C_{147}H_{203}Cl_7N_{30}O_{26}S$) C, H, N. ^{1}H NMR (500 MHz, DMSO-d_6): δ 1.1–1.8 (42H + 28H, m, HNCH$_2$(*CH$_2$*)$_3$ and CH(*CH$_2$*)$_2$), 1.90 (14H, *CH$_2$*(CH$_2$)$_2$CH), 2.9–3.1 (14H, m, HN*CH$_2$*), 3.46 (2H, m, SCNH*CH$_2$*), 4.20 (7H, m, NH*CH*CO), 4.66 (14H, s, br, *CH$_2$*(CH$_2$)$_3$CH), 6.5–6.6 (4H, m, aryl H), 6.68 (2H, s, br, aryl H), 8.26 (7H, dd, br, pyridine), 8.98 (7H, s, br, pyridine), 9.25 (7H, s, br, pyridine), 9.63 (7H, d, br, pyridine).

*Fluorescein-aca-[Lys(Nys$^+$)-aca]$_8$-Lys(Nys$^+$)-NH$_2$ (**3**)*
General procedure E was followed with fluorescein isothiocyanate (26 mg, 0.067 mmol) and amine **26** (0.15 g, 0.043 mmol). Yield 0.09 g (54%). Mp: 160°C. Anal. ($C_{183}H_{257}Cl_9N_{38}O_{32}S$) C, H, N. ^{1}H NMR (500 MHz, DMSO-d_6): δ 1.1–1.7 (54H + 36H, m, HNCH$_2$(*CH$_2$*)$_3$ and CH(*CH$_2$*)$_2$), 1.96 (18H, *CH$_2$*(CH$_2$)$_2$CH), 2.08 (18H, m, CH$_2$CO), 2.9–3.1 (16H, m, HN*CH$_2$*), 3.46 (2H, m, SCNH*CH$_2$*), 4.20 (9H, m, NH*CH*CO), 4.65 (18H, s, br, *CH$_2$*(CH$_2$)$_3$CH), 6.55 (2H, dd, aryl H), 6.58 (2H, d, aryl H), 6.68 (2H, s, br, aryl H), 6.97/7.38 (1H + 1H, s, CHCO*NH$_2$*), 7.14 (1H, d, aryl H), 7.80 (1H, br, aryl H), 8.26 (9H, dd, pyridine), 8.37 (1H, s, br, aryl H), 8.98 (9H, br, pyridine), 9.23 (9H, br, pyridine), 9.60 (9H, br, pyridine). ES-MS: calculated for ($C_{183}H_{257}N_{38}O_{32}S$) 3533.3, found 3532.0.

*Fluorescein-aca-Lys(Nys$^+$)-aca-[Lys(Nys$^+$)-Lys(Nys$^+$)-aca]$_2$-Lys(Nys$^+$)-Lys(Nys$^+$)-NH$_2$ (**4**)*
General procedure E was followed with fluorescein isothiocyanate (35 mg, 0.09 mmol) and amine **34** (0.14 g, 0.06 mmol). Yield 0.098 g (60%). Mp: 175°C. Anal. ($C_{129}H_{170}Cl_7N_{27}O_{23}S$) C, H, N. ^{1}H NMR (500 MHz, DMSO-d_6): δ 1.1–1.7 (24H + 28H, m, HNCH$_2$(*CH$_2$*)$_3$ and CH(*CH$_2$*)$_2$), 1.97 (14H, *CH$_2$*(CH$_2$)$_2$CH), 2.09 (8H, m, CH$_2$CO), 2.9–3.1 (6H, m, HN*CH$_2$*), 3.45 (2H, m, SCNH*CH$_2$*), 4.20 (7H, m, NH*CH*CO), 4.67 (14H, s, br, *CH$_2$*(CH$_2$)$_3$CH), 6.5–6.6 (4H, m, aryl H), 6.67 (2H, s, br, aryl H), 7.03/7.45 (1H + 1H, s, CHCO*NH$_2$*), 7.14 (1H, d, aryl H), 7.84 (1H, d, br, aryl H), 8.26 (7H, dd, pyridine), 8.41 (1H, s, br, aryl H), 8.99 (7H, br, pyridine), 9.28 (7H, m, pyridine), 9.68 (7H, m, pyridine). ES-MS: calculated for ($C_{129}H_{170}N_{27}O_{23}S$) 2499.0, found 2498.4.

CD and FTIR spectroscopy

The 2,2,2-trifluoroethanol (TFE, 99.5%, NMR grade) used as solvent for the circular dichroism (CD) and Fourier transform infrared (FTIR) measurements was purchased from Aldrich. CD measurements were performed on a Jasco J-810 Dichrograph at room temperature in TFE and water using quartz cell with 0.02-cm path length. The spectra were averages of 5–8 scans in the region 180 and 260 nm. The concentration of peptides was 0.11–0.34 mM. FTIR spectra at a resolution of 2 cm^{-1} in TFE were obtained as average of 256 scans with a Bruker Equinox 55 FTIR spectrometer equipped with a DTGS detector. CaF_2 cells with 0.021-cm path length and sample concentration of 5 mg mL^{-1} were used. The spectra were corrected with the background.

Molecular modelling

Three-dimensional molecular structures used for illustration were built and fully geometry-optimized using AM1 semi-empirical quantum chemical calculations (Dewar et al 1985) in CAChe 5.0 (Fujitsu, Ltd., Chiba, Japan). The electron-iso-density surfaces corresponding to 0.01 electron/Å^3 ≈ 0.0015 electron/bohr^3 shown in Figure 2 were also obtained with this method, and they were colour-coded so as to have blue colours corresponding to the more negative regions and red colours corresponding to the more positive regions along the surface. For the larger compounds, optimized structures were transferred to DS ViewerPro 5.0 (Accelrys, Inc., San Diego, CA) and a transparent soft surface coloured by the electrostatic potential was generated using this software that uses a reversed colour coding with the blue colours corresponding to the more positive regions. Molecular volumes used here as size descriptors were calculated using computer models and software described in our previous publications (Buchwald & Bodor 1999; Buchwald 2002).

Cell culture

HeLa (human cervical carcinoma cells) were cultivated in Dulbecco's modified Eagle medium (DMEM) with glutamax, supplemented with 10% fetal bovine serum, 1% penicillin–streptomycin solution, 1% sodium pyruvate, and 1% non-essential amino acids at 37 °C and 5% CO_2 atmosphere.

Cellular uptake studies

Cells were seeded two days before the experiment in 12 well plates, 100 000 cells/well. Peptides were dissolved in serum-free medium at a concentration of 5 μM and incubated with the cells for 60 min at 37°C. The cells were washed twice with serum-free medium and detached by trypsin treatment for 5 min. After centrifugation at 1000 *g* for 5 min at 4°C, the trypsin was removed and the cells were lysed in 300 μL 0.1 M NaOH for 60 min. The fluorescence of the lysate was measured at 494/518 nm in a fluorescence spectrophotometer. Cellular uptake was normalized against protein amount.

Statistical analysis

Cellular uptake data (triplicates for each compound) were compared against dextran as reference using nonparametric Mann–Whitney *U* (Wilcoxon rank-sum)-tests for the compound-pairs of interest (Jones 2002). $P < 0.05$ denoted significant difference in all cases. All statistical analyses were performed using NCSS 2007 (Number Cruncher Statistical Systems, Kaysville, UT).

Results and Discussion

Chemistry

The novel compounds containing five (**1**), seven (**2**) or nine (**3**) Nys$^+$ units, which to denote their synthetic origin will be denoted as Lys(Nys$^+$) here, together with five, seven, or nine aminocaproic acid units (aca: –NH(CH$_2$)$_5$CO–) separating

each consecutive Nys^+ unit (with aca also present at the *N*-terminal) and a heptamer (**4**) with a modified sequence (Figure 3) have been prepared via solution-phase synthesis. The most effective synthetic pathway was a fragment condensation coupling method starting from Lys(Z)-NH_2 (**6**) using 2,4,5-trichloro-phenyl esters (**5, 10, 28**) (Figure 4, 6). The BOC group was removed under acidic conditions. A 2,2,2-trichloroethyl (TCE) group was used to protect the *C*-terminal of BOC-aca-OH (Frank et al 1977) by using 2,2,2-trichloroethanol, DCC and DMAP to prepare the TCE esters. The TCE protecting group was removed by reduction with zinc dust in acetic acid.

Simultaneous cleavage of the benzyloxycarbonyl groups by catalytic hydrogenolysis led to compounds **18, 19, 20** and **32** (Figure 5, 6). The insolubility of the protected intermediates **11, 14, 17** and **31** in methanol caused difficulties, but hydrogenation in acetic acid was successful. The quaternary pyridinium-3-amide (Nys^+) derivatives were formed via the Zincke reaction (Zincke 1903; Lettré et al 1953; Atkinson et al 1965; Génisson et al 1992; Chen et al 1998). The obtained polyamine compounds were converted into poly Nys^+ **21, 22, 23** and **33** by treatment with excess *N*-(2,4-dinitrophenyl)-pyridinium chloride in good yields (60–85%).

The fluorescein moiety was attached through an aminocaproic acid (aca) spacer at the amino termini. Fluorescent labelling of **24, 25, 26** and **34** was achieved by treatment with 1.5 equivalent of fluorescein isothiocyanate in DMSO. Finally, Sephadex LH 20 purification of the peptide derivatives led to the pure fluorescein-labelled compounds **1, 2, 3** and **4**.

Conformational analysis: CD and FTIR spectroscopy

The CD spectra of **3** and its corresponding Lys analogue (**20**) measured in trifluoroethanol (TFE) and water are presented in Figure 7. The CD spectra in TFE have comparable intensities and somewhat similar shapes, suggesting that the two peptides adopt a more-or-less identical conformation in this solvent. TFE is known to promote the adoption of helical (α-helix or 3_{10} helix) or folded conformations fixed by intramolecular H-bonds (Jackson & Mantsch 1992; Hollósi et al 1994). However, due to the unusual amino-acid sequence resulting from the presence of aca, the spectra of **3** and **20** in TFE cannot be associated with a typical helix or β-sheet conformation of polypeptides built up exclusively from α-amino acids. Adoption of such ordered secondary structures is also disfavoured by the repulsion of the positively charged, bulky Lys^+ and Nys^+ side-chains, respectively. The shape of the CD curves in this solvent reflects the presence of some ordered conformation being compatible with an extended strand structure or γ-turns. Molecular modelling performed in vacuum at the AM1 semi-empirical level for **3** and **20** suggests a mainly extended conformation for the backbone leading to the minimization of

Fl-aca-[Lys(Nys^+)-aca]$_n$-Lys(Nys^+)-NH_2

1 $n = 4$
2 $n = 6$
3 $n = 8$

Fl-aca-Lys(Nys^+)-aca-[Lys(Nys^+)-Lys(Nys^+)-aca]$_2$-Lys(Nys^+)-Lys(Nys^+)-NH_2

4

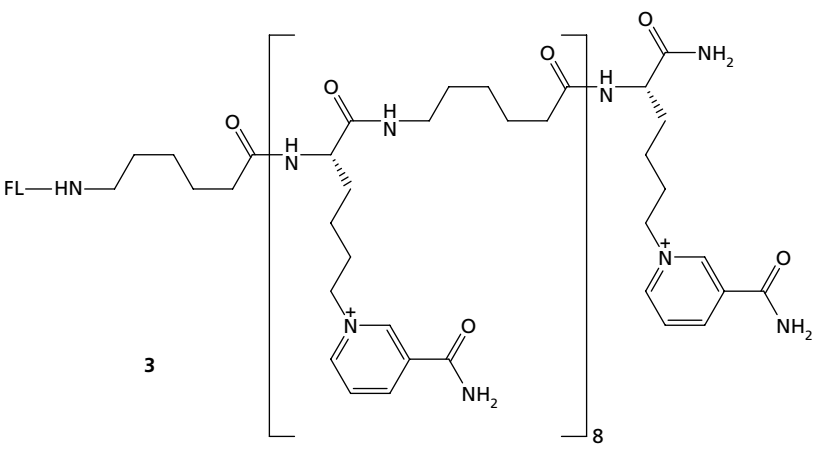

Figure 3 Nys^+-containing compounds prepared for the study.

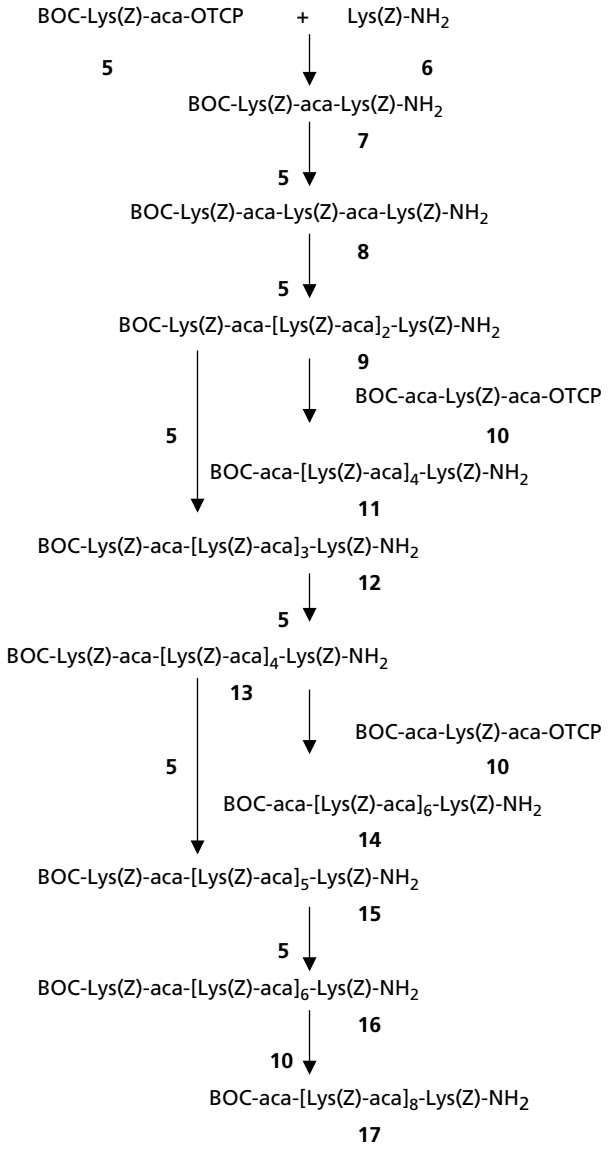

Figure 4 Synthetic pathway (part 1/3).

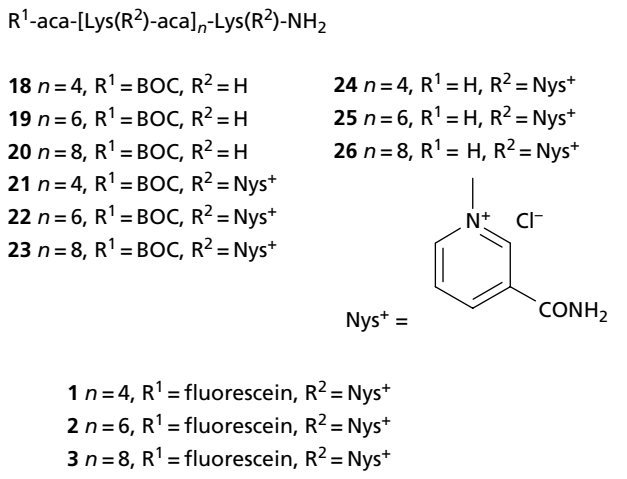

Figure 5 Synthetic pathway (part 2/3).

the side-chain repulsions (Figure 8). Formation of folded structures, such as inverse γ-turns centered at the Lys or Nys residues, stabilized by intramolecular C_7 H-bonds is also possible, while the backbone preserves the mainly extended or slightly zigzag ribbon shape. The spectra measured in TFE and in water differ significantly, as shown by the solid and dashed lines, respectively, in Figure 7. The CD curves recorded in the latter solvent reflect the loss of any ordered conformation, suggesting an unordered structure in aqueous solution.

The infrared spectra of **3** and **20** measured between 1800 and 1500 cm^{-1} in TFE are shown in Figure 9. The amide I band of **20** at 1652 cm^{-1}, with a high-wavenumber shoulder at ~1665 cm^{-1}, is relatively weak. Its position is compatible with highly solvated amide carbonyls, unordered, or repeating folded conformation(s). The weak, higher-wavenumber band at 1710 cm^{-1} is assigned to the CO stretching vibration of the Boc group. The amide II band (1570–1500 cm^{-1}) is rather strong, which is probably due to the overlap with the anti-symmetric stretching vibration band of the acetate counter-ions associated with the protonated Lys side-chains.

The FTIR spectrum of **3** contains separated component bands. Unfortunately, in this case, the Nys side-chain contributions to the amide I region strongly interfere with the vibrations of backbone amides, making the interpretation of the spectrum rather difficult. The sharp and strong band at 1700 cm^{-1} is likely due to the amide I vibration of the primary amide group of Nys^+. The amide I band of the peptide bonds is similar to that of **20**. This finding is compatible with the preservation of the extended strand or repeating folded conformation of **20**. The band at ~1619 cm^{-1} belongs to the amide II vibration of the $CONH_2$ groups of Nys^+, while the weak bands at ~1600 and 1590 cm^{-1} are related to the heteroaromatic ring vibrations of Nys^+. The intensity of the amide II band of **3** is rather weak due to the lack of IR absorption of the Cl^- counter-ions of Nys^+, as opposite to the acetate counterions of **20**, having strong interference with the amide II region.

Cellular uptake

Quantitative uptake characterization was carried out on human cervical carcinoma (HeLa) cells. The cell-penetrating peptide TP10 (AGYLLGKINLKALAALAKKIL) (Soomets et al 2000; Kilk et al 2005) and dextran-FITC, which is not taken up into cells, was included as positive and negative control, respectively. Results (Figure 10) indicated that **1** is not taken up, **2** and **4** are internalized to some extent and **3** has the highest uptake, although less than TP10. About 0.1% of the added **3** was internalized compared with about 4% of the TP10.

The quanidium moiety of Arg may possess a unique affinity toward binding anions (Rothbard et al 2004; Sakai et al 2005); nevertheless, the three-dimensional molecular structures of the novel Nys^+ compounds are very similar to those of the corresponding arginine compounds both in their overall

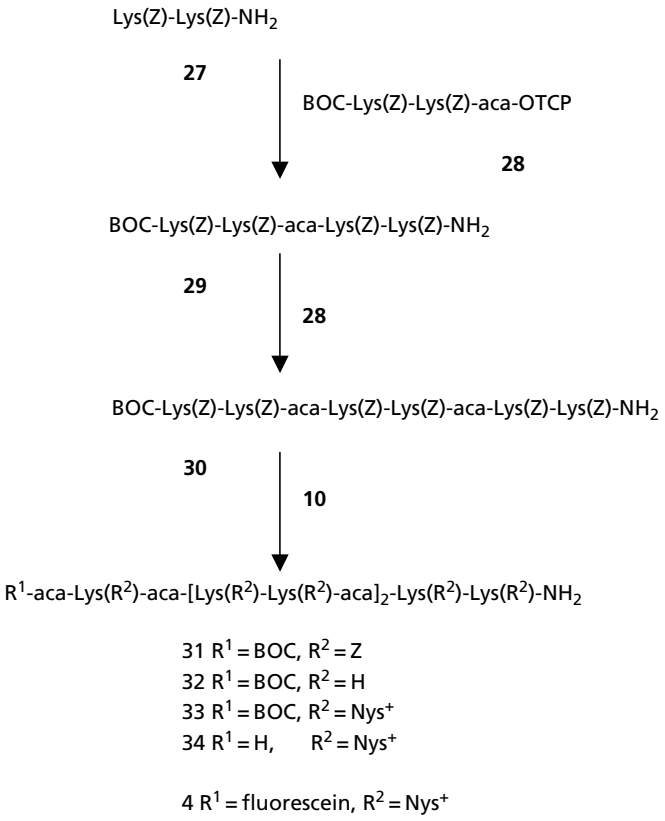

Figure 6 Synthetic pathway (part 3/3).

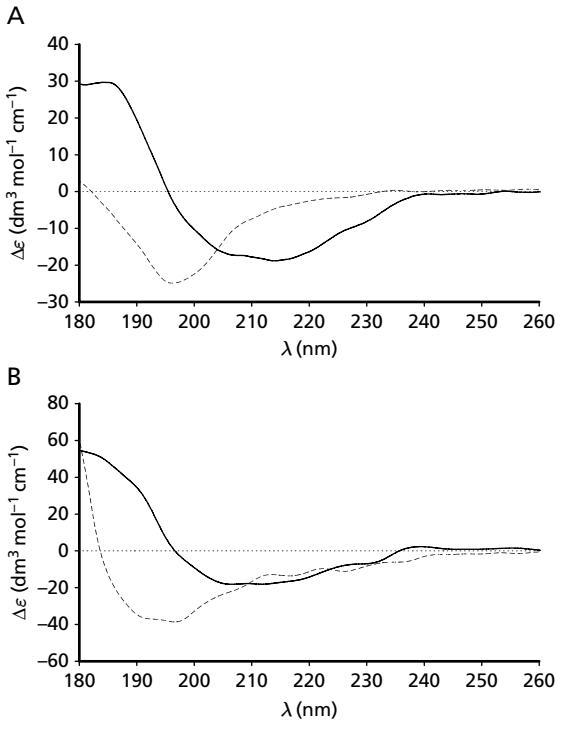

Figure 7 CD spectra of **20** (A) and **3** (B) obtained in TFE and water (solid and dashed lines, respectively).

size and electronic distribution (Figure 8). The permanently charged trigonellyl side chains with their quaternary *N*-heads results in somewhat more diffuse positive charges and slightly larger structures than the arginine- or lysine-containing structures (e.g., calculated molecular volume (Buchwald & Bodor 1999; Buchwald 2002), *V* of 2495.8 Å^3 for the Nys$^+$-containing **3** vs 1974.8 Å^3 for its Arg$^+$ analogue and 1850.8 Å^3 for its Lys$^+$ analogue **20**; all of them without their ending fluorescein or Boc moieties), but otherwise a good analogy is maintained. Because of their sufficiently elongated side-chains and their aca-spaced backbone structures, they also maintain the flexibility that seems necessary for adequate cellular uptake (Figure 8). In fact, such a structure, somewhat resembling a caterpillar with diffuse, positively charged 'legs' corresponding to the quaternary guanidine or trigonellyl moieties, seems well-suited to 'crawl' along the cellular wall following concentration or electrical gradients by 'stepping' along negatively charged phosphate groups and to pair up with these negative charges, a neutralization process that may enhance its uptake by endocytosis or some other mechanism.

Conclusions

New analogues of arginine-rich cell-penetrating molecular transporters have been prepared by incorporation of a novel redox amino acid (Nys$^+$). A nonamer analogue (**3**) with a caterpillar-like structure showed transporter activity, resulting in increased cellular uptake in human carcinoma (HeLa) cells.

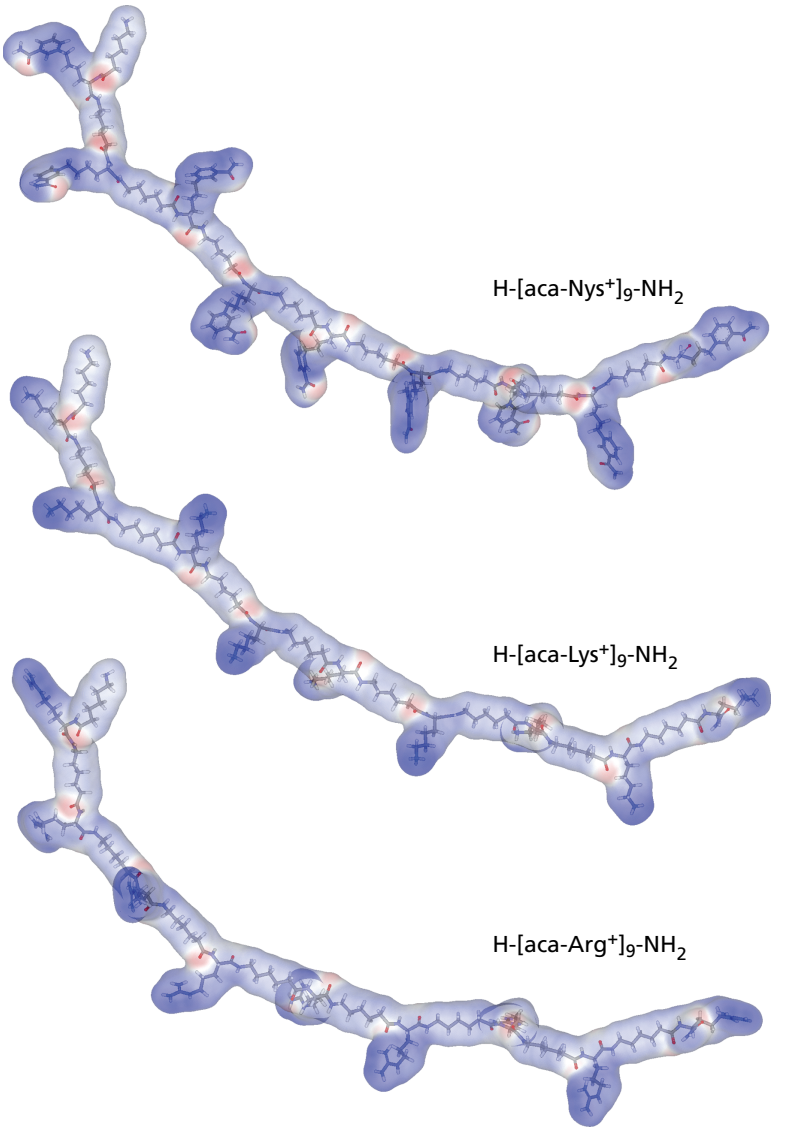

Figure 8 AM1-optimized structure of **3** (without its fluorescein moiety, H-[aca-Nys$^+$]$_9$-NH$_2$) and its Lys$^+$ (**20** without Boc, H-[aca-Lys$^+$]$_9$-NH$_2$) and Arg$^+$ analogues covered with soft, transparent surfaces coloured according to the electrostatic potential. This time, more blue colours correspond to more positive regions.

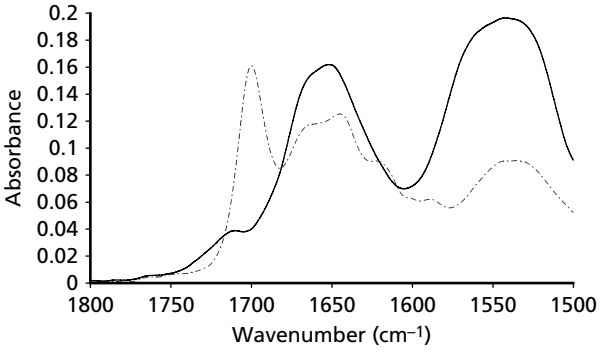

Figure 9 FTIR spectra of **20** and **3** recorded in TFE (solid and dashed lines, respectively).

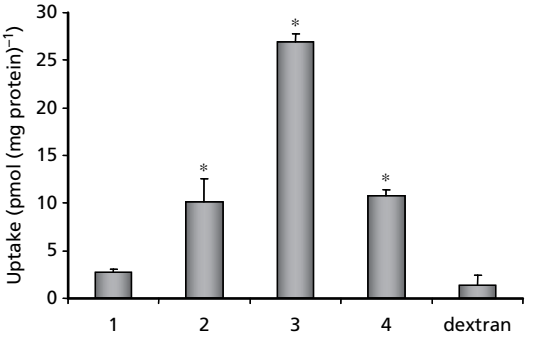

Figure 10 Quantitative uptake of the Nys$^+$-containing compounds **1**–**4** in human cervical carcinoma (HeLa) cells. *$P < 0.05$ compared with dextran (Mann–Whitney *U*- or Wilcoxon rank-sum test).

The unusual cell-penetrating ability of such compounds could, at least partially, be due to their peculiar structure with an elongated backbone and flexible positively charged leg-like side chains.

References

Aarts, M., Liu, Y., Liu, L., Besshoh, S., Arundine, M., Gurd, J. W., Wang, Y.-T., Salter, M. W., Tymianski, M. (2002) Treatment of ischemic brain damage by perturbing NMDA receptor-PSD-95 protein interactions. *Science* **298**: 846–850

Atkinson, M. R., Morton, R. K., Naylor, R. (1965) Synthesis of glycosylpyridinium compounds from glycosylamines and from glycosyl halides. *J. Chem. Soc*. 610–615

Bodor, N., Buchwald, P. (2003a) Brain-targeted delivery: experiences to date. *Am. J. Drug Deliv*. **1**: 13–26

Bodor, N., Buchwald, P. (2003b) Retrometabolism-based drug design and targeting. In: Abraham, D. J. (ed.) *Burger's medicinal chemistry and drug discovery. Vol. 2, Drug discovery and drug development*. 6th Edn, Wiley, New York, pp 533–608

Buchwald, P. (2002) Complexation thermodynamics of cyclodextrins in the framework of a molecular size-based model for nonassociative organic liquids that includes a modified hydration-shell hydrogen-bond model for water. *J. Phys. Chem. B* **106**: 6864–6870

Buchwald, P., Bodor, N. (1999) Quantitative structure-metabolism relationships: steric and nonsteric effects in the enzymatic hydrolysis of noncongener carboxylic esters. *J. Med. Chem.* **42**: 5160–5168

Calnan, B. J., Tidor, B., Biancalana, S., Hudson, D., Frankel, A. D. (1991) Arginine-mediated RNA recognition: the arginine fork. *Science* **252**: 1167–1171

Chen, P., Bodor, N., Wu, W.-M., Prokai, L. (1998) Strategies to target kyotorphin analogues to the brain. *J. Med. Chem*. **41**: 3773–3781

Deshayes, S., Morris, M. C., Divita, G., Heitz, F. (2005) Cell-penetrating peptides: tools for intracellular delivery of therapeutics. *Cell. Mol. Life Sci*. **62**: 1839–1849

Dewar, M. J. S., Zoebisch, E. G., Healy, E. F., Stewart, J. J. P. (1985) AM1: a new general purpose quantum mechanical molecular model. *J. Am. Chem. Soc*. **107**: 3902–3909

El-Andaloussi, S., Holm, T., Langel, Ü. (2005) Cell-penetrating peptides: mechanisms and applications. *Curr. Pharm. Des*. **11**: 3597–3611

Fernández-Carneado, J., Van Gool, M., Martos, V., Castel, S., Prados, P., de Mendoza, J., Giralt, E. (2005) Highly efficient, nonpeptidic oligoguanidinium vectors that selectively internalize into mitochondria. *J. Am. Chem. Soc*. **127**: 869–874

Frank, J., Kriwaczek, V. M., Marchand, C., Schwyzer, R. (1977) ε-Aminocaproylcholine: chemical synthesis, biological properties, and interactions with receptor molecules. *Helv. Chim. Acta* **60**: 2551–2558

Génisson, Y., Marazano, C., Mehmandoust, M., Gnecco, D., Das, B. C. (1992) Zincke reaction with chiral primary amines — a practical entry to pyridinium salts of interest in asymmetric-synthesis. *Synlett* 431–434

Hollósi, M., Majer, Z., Rónai, A. Z., Magyar, A., Medzihradszky, K., Holly, S., Perczel, A., Fasman, G. D. (1994) CD and Fourier transform IR spectroscopic studies of peptides. II. Detection of beta-turns in linear peptides. *Biopolymers* **34**: 177–185

Jackson, M., Mantsch, H. H. (1992) Halogenated alcohols as solvents for proteins: FTIR spectroscopic studies. *Biochim. Biophys. Acta* **1118**: 139–143

Jones, D. S. (2002) *Pharmaceutical statistics*. Pharmaceutical Press, London

Jones, S. W., Christison, R., Bundell, K., Voyce, C. J., Brockbank, S. M., Newham, P., Lindsay, M. A. (2005) Characterisation of cell-penetrating peptide-mediated peptide delivery. *Br. J. Pharmacol*. **145**: 1093–1102

Kilk, K., El-Andaloussi, S., Järver, P., Meikas, A., Valkna, A., Bartfai, T., Kogerman, P., Metsis, M., Langel, Ü. (2005) Evaluation of transportan 10 in PEI mediated plasmid delivery assay. *J. Control. Release* **103**: 511–523

Lettré, H., Haede, W., Ruhbaum, E. (1953) Zur Darstellung von Derivaten des Nicotinsäureamids. *Ann. Chem*. **579**: 123–132

Lindgren, M., Hällbrink, M., Prochiantz, A., Langel, Ü. (2000) Cell-penetrating peptides. *Trends Pharmacol. Sci*. **21**: 99–103

Rothbard, J. B., Garlington, S., Lin, Q., Kirschberg, T., Kreider, E., McGrane, P. L., Wender, P. A., Khavari, P. A. (2000) Conjugation of arginine oligomers to cyclosporin A facilitates topical delivery and inhibition of inflammation. *Nat. Med*. **6**: 1253–1257

Rothbard, J. B., Kreider, E., VanDeusen, C. L., Wright, L., Wylie, B. L., Wender, P. A. (2002) Arginine-rich molecular transporters for drug delivery: role of backbone spacing in cellular uptake. *J. Med. Chem*. **45**: 3612–3618

Rothbard, J. B., Jessop, T. C., Lewis, R. S., Murray, B. A., Wender, P. A. (2004) Role of membrane potential and hydrogen bonding in the mechanism of translocation of guanidinium-rich peptides into cells. *J. Am. Chem. Soc*. **126**: 9506–9507

Rousselle, C., Clair, P., Lefauconnier, J.-M., Kaczorek, M., Scherrmann, J.-M., Temsamani, J. (2000) New advances in the transport of doxorubicin through the blood-brain barrier by a peptide vector-mediated strategy. *Mol. Pharmacol*. **57**: 679–686

Sakai, N., Takeuchi, T., Futaki, S., Matile, S. (2005) Direct observation of anion-mediated translocation of fluorescent oligoarginine carriers into and across bulk liquid and anionic bilayer membranes. *Chembiochem* **6**: 114–122

Santana, A., Hyslop, S., Antunes, E., Mariano, M., Bakhle, Y. S., de Nucci, G. (1993) Inflammatory responses induced by poly-L-arginine in rat lungs in vivo. *Agents Actions* **39**: 104–110

Schwarze, S. R., Ho, A., Vocero-Akbani, A., Dowdy, S. F. (1999) In vivo protein transduction: delivery of a biologically active protein into the mouse. *Science* **285**: 1569–1572

Soomets, U., Lindgren, M., Gallet, X., Hällbrink, M., Elmquist, A., Balaspiri, L., Zorko, M., Pooga, M., Brasseur, R., Langel, Ü. (2000) Deletion analogues of transportan. *Biochim. Biophys. Acta* **1467**: 165–176

Takagi, H., Shiomi, H., Ueda, H., Amano, H. (1979) A novel analgesic dipeptide from bovine brain is a possible Met-enkephalin releaser. *Nature* **282**: 410–412

Tyagi, M., Rusnati, M., Presta, M., Giacca, M. (2001) Internalization of HIV-1 tat requires cell surface heparan sulfate proteoglycans. *J. Biol. Chem*. **276**: 3254–3261

Vivès, E., Brodin, P., Lebleu, B. (1997) A truncated HIV-1 Tat protein basic domain rapidly translocates through the plasma membrane and accumulates in the cell nucleus. *J. Biol. Chem*. **272**: 16010–16017

Wender, P. A., Mitchell, D. J., Pattabiraman, K., Pelkey, E. T., Steinman, L., Rothbard, J. B. (2000) The design, synthesis, and evaluation of molecules that enable or enhance cellular uptake: peptoid molecular transporters. *Proc. Natl Acad. Sci. USA* **97**: 13003–13008

Wright, L. R., Rothbard, J. B., Wender, P. A. (2003) Guanidinium rich peptide transporters and drug delivery. *Curr. Protein Pept. Sci*. **4**: 105–124

Zincke, T. (1903) Über Dinitrophenylpyridiniumchlorid und dessen Umwandlungsproducte. *Ann. Chem*. **330**: 361–374

Zorko, M., Langel, Ü. (2005) Cell-penetrating peptides: mechanism and kinetics of cargo delivery. *Adv. Drug Deliv. Rev*. **57**: 529–545